Intelligent Control Rod Selection Algorithm for Core Power Control at TRIGA PUSPATI Reactor Using Fuzzy Logic Technique

S. Gunasegaran[1], A. C. Soh[1*], R. Z. A. Rahman[1], M.S. Minhat[2]
[1]Department of Electrical and Electronic Engineering, Faculty of Engineering,
Universiti Putra Malaysia, 43400, Serdang, Selangor, Malaysia
[2]Reactor Instrumentation and Control Engineering, Reactor Technology Centre,
Malaysia Nuclear Agency, Bangi, 43000 Kajang, Selangor, Malaysia
[*]corresponding author's email: azuracs@upm.edu.my

Abstract – *The TRIGA PUSPATI Reactor (RTP) serves as Malaysia's primary research reactor, supporting a range of nuclear applications. A critical element in its operation is the control rod selection algorithm (CRSA), which regulates reactor power and ensures stability. The conventional CRSA (cCRSA), however, faces challenges in managing transient operations and achieving precise steady-state control due to fluctuations in control rod worth. To address these issues, a new fuzzy logic-based control rod selection algorithm (Fuzzy-CRSA) has been developed and validated through MATLAB simulations. This Fuzzy-CRSA approach provides a more flexible and resilient method for controlling the reactor's four types of rods. By optimizing rod selection and movement, Fuzzy-CRSA achieves faster response times and greater stability compared to the cCRSA, with improvements in rise time from 0.57% to 27.67% and in settling time from 3.14% to 25.88%. These results highlight Fuzzy-CRSA's capability to more effectively meet the RTP's power requirements, enhancing reactor performance and supporting Malaysia's nuclear research progress.*

Keywords: *control rod selection, control rod sequence, core power control, fuzzy logic, research reactor*

Article History
Received 13 November 2024
Received in revised form 26 December 2024
Accepted 17 January 2025

I. Introduction

Malaysia's sole research reactor, the TRIGA PUSPATI Reactor (RTP) of the Mark II type, has been operated by the Malaysian Nuclear Agency since its commissioning on June 28, 1982. The acronym TRIGA represents its functions: Training, Research, Isotope Production, and General Atomic. This reactor, with a nominal power output of 1 MW, is instrumental in supporting a wide array of nuclear research, services, and training. Over the years, it has primarily been used for neutron activation analysis (NAA) experiments, alongside applications in neutron radiography, small-angle neutron scattering (SANS), and the production of isotopes for tracer studies [1].

In nuclear reactor kinetics, the operational characteristics of a power reactor are influenced by changes in temperature and the positioning of control rods. These changes result from variations in temperature and neutron absorption rates [2]. Control rods within the reactor core absorb neutrons; as they are withdrawn, neutron absorption decreases, allowing reactor power to rise and potentially pushing the reactor toward a supercritical state. Conversely, inserting the control rods increases neutron absorption, thus reducing reactor power and moving it toward a subcritical state. When reactor power stabilizes, it reaches a critical state. Maintaining this power level involves continuously adjusting the control rods up and down as needed [3].

Strategies for control rod movement differ between research and power reactors. In research reactors, single-rod control is often employed, where only one control rod is adjusted at a time. In contrast, power reactors generally utilize a banked approach, moving multiple control rods simultaneously to manage the reactor's neutron flux or power level [4]. These control rods are

This is an Open Access article distributed under the terms of the Creative Commons Attribution-Noncommercial 3.0 Unported License, permitting copy and redistribution of the material and adaptation for commercial and uncommercial use.

usually made of materials like boron, cadmium, gadolinium, or hafnium, which are highly effective at absorbing neutrons. Their positions are regulated by a control rod drive system, allowing for changes in the thermal utilization factor.

At peak power, the control rods are fully withdrawn. Operators primarily use control rods to manage reactor trips, adjust power levels, and respond to fast-changing reactivity transients. Unlike generating reactors, research reactors use control rods differently. Research reactors typically lack chemical shim control, so they rely on control rods for coarse, fine, or quick shutdowns, as well as to compensate for short-term reactivity effects caused by fission product poisons, among other factors. Consequently, the position of the control rods may vary significantly during a single operational cycle. This necessitates the use of single rod control for control rod movements in research reactors [5].

The RTP features four control rods—Transient (TR), Safety (SF), Shim (SH), and Regulating (RG)—each with distinct roles in maintaining reactor stability. The CRSA determines rod movement, operating within specific speed limits to adjust reactor power. In the cCRSA, the rod with the lowest position or worth value is selected for movement, minimizing travel distance in a method known as balancing position control. While this approach maintains a chattering error of 2%, it struggles with transient conditions and steady-state fine-tuning due to fluctuating rod worth values at RTP [6].

Another type of conventional CRSA method is discussed in [7] for the Egyptian Second Testing Research Reactor (ETRR-2). Unlike traditional approaches that select the control rod with the lowest position for withdrawal, this method prioritizes the control rod with the lowest worth value to increase reactor power, and vice versa. Consequently, the control rod positions will vary, as each control rod has a different worth value. However, this rod selection strategy may not yield consistent results for RTP due to the significant disparity between the minimum and maximum control rod worth value.

Both conventional CRSA methods (RTP and ETRR-2) face limitations in making optimal decisions for controlling power in nuclear reactors. Furthermore, the controller's actions in these methods are solely derived from the error equation, with the controller's output (velocity) sent directly to the CRSA system without accounting for the dynamic behavior of the control rods. As a result, the tracking performance is compromised, as conventional CRSA approaches rely exclusively on either rod positions or rod worth values to manage the operation of all four control rods.

An intelligent fuzzy logic-based approach is proposed to enhance the transient response and overall performance of control rod selection in RTP control. This Fuzzy-CRSA leverages advancements in Artificial Intelligence (AI) aligned with the Fourth Industrial Revolution (IR4.0), enabling adaptive, autonomous adjustments based on real-time system conditions and control rod worth values. Unlike conventional CRSA (cCRSA) methods, the fuzzy logic system introduces AI-driven independence and responsiveness, dynamically identifying optimal control rod combinations and movements to meet power demands effectively.

The suitability of fuzzy control lies in its ability to handle nonlinear system characteristics, which are inherent in reactor dynamics. Traditional control methods often struggle with these complexities, as they rely heavily on linear approximations or predefined control strategies that may not adapt well to varying operational conditions. In contrast, fuzzy controllers excel in managing systems with uncertainty and imprecision, making them ideal for real-time applications. However, designing fuzzy controllers is not straightforward, as it requires careful tuning of membership functions and rule sets to ensure optimal performance.

The proposed Fuzzy-CRSA is anticipated to effectively manage rod selection and has the potential to enhance RTP functionality and efficiency, aligning with IR4.0's objectives of process optimization and operational excellence [8]. By tackling the complexities of control rod selection through a fuzzy logic-based framework, this approach promotes sustainable and efficient reactor operation while advancing cutting-edge methodologies in nuclear power control.

II. Methodology

The initial phase of this project involves researching the current approach for control rod movement in the RTP reactor, which relies on the cCRSA. The cCRSA manages four control rods by selecting the rod at the lowest position for withdrawal, regardless of rod worth. This sequential withdrawal achieves the target power of 1 MWth, but lacks an optimized approach based on rod position or worth, limiting operational efficiency.

A block diagram as show in Fig. 1 illustrates cCRSA's flow, where distance values are input to the CRSA block to determine rod position. This position is converted to height through the Control Rod Drive Mechanism (CRDM) and then into reactivity before

entering the plant model, which consists of neutronics, thermal hydraulics, and reactivity subsystems. From this model, the reactor's power output is derived based on the reactivity values.

To enhance efficiency, this project will develop an automatic rod selection technique using fuzzy logic, known as the Fuzzy-CRSA system, to replace the manual cCRSA approach. The Fuzzy-CRSA system will prioritize control rods for withdrawal, with efficiency measured by the time taken to reach the target output of 1 MWth. Due to safety limitations, testing and comparison between the cCRSA and fuzzy logic approaches will be conducted through simulations. These results will determine the most effective rod selection algorithm for implementation in RTP. This project is currently focused solely on control rod withdrawal for power gain.

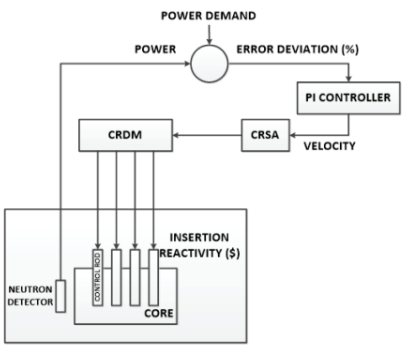

Fig. 1. Block diagram of cCRSA block diagram in RTP[6].

A. RTP Model

The reactor model for RTP utilized in this project is a nonlinear representation, encompassing three primary subsystems: the neutronics model, the thermal-hydraulic model, and the reactivity model as shown in Fig. 2.

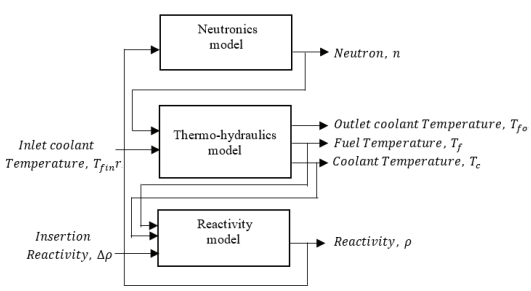

Fig. 2. Block diagram of reactor model [3].

Neutronics Model: The neutronics model describes the chain reaction initiated when a neutron collides with a U-235 nucleus, resulting in absorption and subsequent fission, which produces additional 'child' neutrons. These newly formed neutrons, in turn, initiate further reactions by interacting with other nuclei, perpetuating the process. This neutron generation, combined with delayed neutron precursors, is captured by the point reactor kinetics equations, which describe the dynamic behavior of neutron populations. The point reactor kinetics equation with six groups of delayed neutron precursor is defined as [9], [10]:

$$\frac{dn(t)}{dt} = \left[k_{eff}(1-\beta) - 1\right]\frac{n(t)}{\Lambda} + \sum_{i=1}^{6} \lambda_i C_i(t) \qquad (1)$$

Where $i = 1..6,;\ \beta = \sum_{i=1}^{6} \beta_i$;

$$\frac{dC(t)}{dt} = k_{eff}\beta_i \frac{n(t)}{\Lambda} - \lambda_i C_i(t) \qquad (2)$$

By referring to the equation the above equation can be expressed as:

$$\frac{dn(t)}{dt} = \frac{\rho(t)-\beta}{\Lambda} n(t) + \sum_{i=1}^{6} \frac{\beta_i}{\Lambda} C_i(t) \qquad (3)$$

$$\frac{dC_i(t)}{dt} = C_i n(t) - C_i n_i(t);\ \ i = 1, \dots, 6 \qquad (4)$$

Where n is the number of neutrons, C_i is the number of delayed neutrons precursor in group i, β_i is the delayed neutron fraction of group i, λ_i is decay constant for delayed neutron precursor of group i, k_{eff} is the effective multiplication factor and Λ is prompt neutron lifetime also called mean neutron generation time.

Thermal-Hydraulic Model: The second subsystem focuses on thermal and hydraulic behaviors. It takes input from the neutronics model and considers parameters like the inlet coolant temperature T_{fin} while outputting variables such as the outlet coolant temperature T_{fo}, fuel temperature T_f, and coolant temperature T_c. This model provides essential data for understanding the heat transfer and fluid dynamics within the reactor, which are critical for maintaining safety and operational efficiency. The governing equations for this model include [11],[12],[13]:

$$\frac{dT_m}{dt} = \frac{P(1-f)}{\tau_m K} + \frac{T_f - T_m}{\tau_m} - \frac{\Gamma C_m}{\tau_m K}(T_m - T_{in}) \qquad (5)$$

$$\frac{dT_f}{dt} = \frac{P_f}{\tau_f K} - \frac{T_f - T_m}{\tau_f} \quad (6)$$

$$T_m = wT_{out} + (1 - w)T_{in} \quad (7)$$

Additionally, the mass flow rate equation is represented as

$$\Gamma = \frac{K_w(T_f - T_m)}{C_m(T_m - T_{m)}} \quad (8)$$

Reactivity Model: The third subsystem integrates fuel temperature T_f, coolant temperature T_c, and reactivity insertion Δp to calculate the overall reactivity p. The reactivity model is vital for power regulation and stability within the reactor. The equation for reactivity is expressed as [9]:

$$\rho = \alpha_h \Delta h_{cr} + \alpha_m(T_m - T_m^0) + \alpha_f(T_f - T_f^0) \quad (9)$$

In this model, the reactivity output is used to control the reactor power, influencing its performance and ensuring optimal operation. Simulating these models collectively helps predict the reactor's response and enables detailed analysis of its dynamic behavior.

B. Control Rod Selection Algorithm based on Fuzzy Logic Techniques

Implementing a fuzzy logic-based Control Rod Selection Algorithm (Fuzzy-CRSA) in this process allows the system to identify the optimal sequence for withdrawing control rods. The fuzzy logic design uses 'Error' and 'Rate of Error' as input variables, with an output range from 1 to 4, each corresponding to a specific control rod: Regulating, Shim, Safety, or Transient. Here, 'Error' is the difference between the setpoint and actual output, while 'Rate of Error' is determined by dividing the error by the sampling rate. The design rules are based on conditions specified by RTP engineers, who select the appropriate control rod depending on the error and rate of error to ensure stable, smooth, and safe withdrawal. Fig. 3 illustrates the RTP block diagram with Fuzzy-CRSA.

Table I provides detailed descriptions of the membership functions for the 'Error' and 'Rate of Error' inputs, as well as for the 'Control Rods' output. The 'Error' input is defined over five ranges on a scale of 0 to 100, with triangular membership functions chosen for their simplicity and clarity. These functions are evenly distributed, which aids in easy interpretation. The 'Rate of Error' input, ranging from 0 to 12.5 errors per second, also uses a triangular membership function, capped at an upper limit for precision. For the output, representing control rod selection, the same triangular function was applied for consistency. The output ranges from 1 to 4, corresponding to the control rod worth values.

The Fuzzy-CRSA selects control rods based on predefined rules and membership functions, optimizing reactor power control. The rule base, as shown in Table II, was developed by analyzing the control rod characteristics and subsequently validated through rigorous testing. This rule base prioritizes control rods according to their worth values, which represent the ability of each rod to affect the reactor's power level. Specifically, the RG has the highest worth, enabling the fastest power increase, followed by the SF and SH, which have progressively lower worth values. Lastly, the TR, with the lowest worth, offers the slowest power increase, making it ideal for fine power adjustments.

TABLE I
THE INPUT AND OUTPUT PARAMETERS FOR THE FUZZY-CRSA

PARAMETER	MEMBERSHIP FUNCTION/VALUE
INPUT – ERROR	TOO LOW [0 1.5 3] LOW [1.5 13.25 25] MEDIUM-HIGH [15 37.5 60] HIGH [40 65 90] TOO HIGH [85 92.5 100]
INPUT – RATE OF ERROR	SLOW [0 0.75 1.5] MEDIUM [1 2 3] HIGH [2.5 3.6 4.7] TOO HIGH [4 8.25 12.5]
OUTPUT-CONTROL ROD	TR [0 0.6125 1.25] SH [0.5 1.25 2] SF [1.5 2.25 3] RG [2.5 3.25 4]

TABLE II
FUZZY RULES FOR THE FUZZY-CRSA

ERROR		RATE OF ERROR			
		SLOW	MEDIUM	FAST	TOO FAST
		RG	SF	SH	TR
TOO LOW	SH	RG	SH	SH	TR
LOW	SH	SH	SH	SH	SH (0.5) SF (0.25)
MEDIUM-HIGH	SF	SF	SF	SF	SF
HIGH	SF	SF	SF	SF	SF (0.5) RG (0.25)
TOO HIGH	RG	RG	RG	RG	RG

During rapid power increases, the CRSA prioritizes the RG, while the TR is selected for gradual adjustments when error rates are high. Adjustments to the rule base ensure safe and efficient system operation by smoothly transitioning among control rods as error rates and required adjustments change. Specifically, the RG is retained at high error levels, with a shift to SF and SH as

errors decrease, enabling efficient control. Additionally, fine-tuning weightages for specific scenarios, such as "High" or "Low" errors with varying error rates, promotes seamless transitions, minimizing the time required to reach the target power level while maintaining safety and performance.

It is essential to clarify the relationship between rod worth values and rod positions. Rod worth reflects the reactivity contribution of a control rod based on its position in the reactor core. This means that rod worth is not the same as rod position but rather depends on it. The output of the fuzzy logic system, as illustrated in Fig. 3, is the rod position, which specifies the physical movement of the control rods. Meanwhile, rod worth is typically a dimensionless value or a unit associated with reactivity, serving as a guiding parameter in determining which control rods to prioritize. The term 'rod worth' in the context of nuclear reactors refers to the reactivity change caused by inserting or withdrawing control rods. While rod worth is commonly expressed in units such as dollars ($), cents, or pcm (per cent mille), it can also be represented in a unitless form when normalized to the system's effective delayed neutron fraction (β_eff).

The discrepancy in units arises because the rule base uses rod worth as a criterion for decision-making, while the output of the fuzzy logic controller is the rod position, which directly controls the physical adjustments. The conversion between these parameters relies on pre-defined calibration or mapping, ensuring that the fuzzy logic controller appropriately translates reactivity-based priorities into precise rod movements. This dual consideration of rod worth and rod position highlights the robustness of the fuzzy logic system in managing control rod operations, ensuring both rapid response and fine-tuned adjustments for optimal reactor performance.

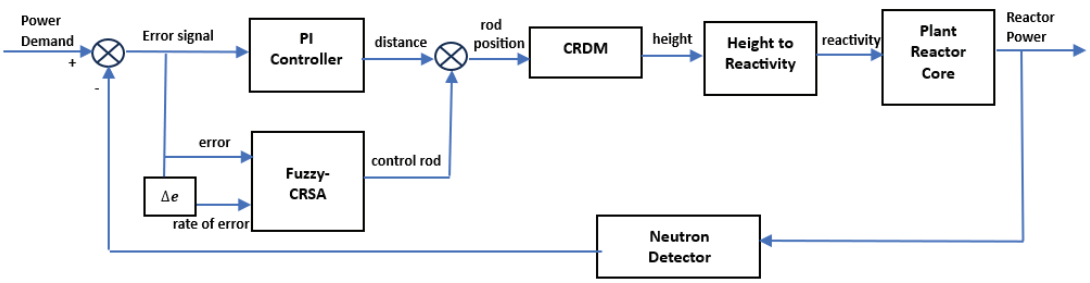

Fig. 3. Block diagram of RTP with Fuzzy-CRSA.

III. Simulation Results and Discussions

This section presents the results of implementing the Fuzzy-CRSA and compares its performance with the current cCRSA method used at RTP. The analysis evaluates control rod movement for both methods, focusing on power distribution and control rod selection to assess their effectiveness. Five design-of-experiment trials were conducted to compare the performance of the cCRSA and Fuzzy-CRSA control rod selection and movement strategies. The simulations evaluated responses at five different power demand levels, ranging from 20% to 100%, starting from an initial power level of 1%. Each simulation was run independently with a stop time of 5,000 seconds and a sampling rate of 0.2 seconds. Step response parameters were analyzed. The performance comparison between Fuzzy-CRSA and cCRSA at various power demand levels is presented in Fig. 4, with a summary of the results provided in Table III

For 100% power demand, the Fuzzy-CRSA exhibited a slight advantage in rise time, responding 5.7 seconds (0.57%) faster than the cCRSA. This small difference highlights the Fuzzy-CRSA's quick response capability, showing comparable performance to the cCRSA method with room for further enhancement. However, the Fuzzy-CRSA had a slower settling time by 39.8 seconds (2.26%), suggesting that while the cCRSA stabilizes more quickly and demonstrates slightly better tracking of power demand profiles, the difference remains minor. This discrepancy was influenced by a brief spike and drop observed in the Fuzzy-CRSA's response. In terms of peak time, the Fuzzy-CRSA system lagged by only 0.4 seconds, reflecting nearly identical performance.

The Fuzzy-CRSA system showed a marginally higher overshoot than the cCRSA method, differing by only (4.39667×10^{-6})%, an almost negligible amount. Overshoot, which represents the maximum deviation from the steady-state value before settling, was minimal and nearly zero. The Fuzzy-CRSA's faster response and

enhanced dynamic properties could offset this minor overshoot. Overall, for 100% power demand, the Fuzzy-CRSA offers only a slight advantage in rise time but is 2.26% slower in settling time compared to the cCRSA.

At the 80% power demand, the Fuzzy-CRSA system demonstrated a notable improvement, responding 81.4 seconds (7.55%) faster in rise time, highlighting its ability to quickly adapt to power demand changes. Additionally, it achieved a 59.4-second (3.14%) faster settling time, indicating quicker stabilization. No difference was observed in peak time between the two systems. The faster rise and settling times of the Fuzzy-CRSA emphasize its speed advantage over the cCRSA at the 80% power demand, even without the initial benefit observed at 100% power. The difference in overshoot between the two systems at this power level was minimal, at just (3.2523×10^{-7}) % negligible amount. This does not detract from the overall superior response of the Fuzzy-CRSA at the 80% power demand level.

At a 60% power demand, the Fuzzy-CRSA achieved a rise time that was 94.1 seconds (8.10%) faster, indicating a quick response to changes in power requirements. It also reached steady-state 165.2 seconds (8.00%) faster, demonstrating quicker stabilization. Both systems had the same peak time, reaching maximum output at 4,999.9 seconds. The Fuzzy-CRSA's improved rise and settling times contribute to enhanced transient response and stability in fine-tuning during steady-state. Although the Fuzzy-CRSA exhibited slightly higher overshoot, approximately 35.69% more than the conventional method, this increase is negligible due to the minimal overshoot value. Overall, the Fuzzy-CRSA showed superior performance at 60% power demand.

At a 40% target power level, the Fuzzy-CRSA system demonstrated a 142-second (10.95%) faster rise time, underscoring its ability to respond quickly to changes in power demand and reduce the time required to stabilize at the new operating point. Additionally, the Fuzzy-CRSA was 304.3 seconds (13.29%) faster in settling time, achieving a quicker steady state. The Fuzzy-CRSA system exhibited a similar peak time to the cCRSA method, as both systems reached their highest point at 4.9999×10^{3}seconds, consistent with previous responses.

The overshoot of the Fuzzy-CRSA was slightly higher, at 4.23% more than that of the cCRSA method. However, given the very low magnitude of this difference, it has no meaningful impact on system stability or steady-state performance. Overall, the Fuzzy-CRSA continued to outperform the cCRSA method at 40% power demand.

For 20% target power, the findings reveal notable advantages of the Fuzzy-CRSA over the cCRSA system in various response aspects. One major advantage is its significant improvement in rise time, outperforming the cCRSA system by 401.6 seconds (27.67%). This demonstrates the Fuzzy-CRSA's ability to adapt swiftly to power demand changes, exhibiting faster response times. Furthermore, the Fuzzy-CRSA achieved 25.88% faster settling time, allowing it to reach a stable state more quickly and achieve the desired power output faster than the cCRSA system. The peak time for both systems remained identical at 4.9999×10^{3} seconds. Even at 20% power demand, where the Fuzzy-CRSA lacked an initial advantage, it still responded significantly faster than the conventional system.

These results emphasize the advantages of the Fuzzy-CRSA over the conventional system. The Fuzzy-CRSA consistently exhibited enhanced responsiveness, with faster rise and settling times across various power demands, demonstrating its effectiveness and efficiency in adapting to power requirements. Although the Fuzzy-CRSA system's overshoot was slightly higher than that of the conventional system at 2.7796×10^{-6} relatively minor difference it remains highly reliable and stable. In summary, the Fuzzy-CRSA system's consistently faster response times confirm its superiority over the conventional system, making it the preferred choice for effectively and efficiently meeting power demand requirements across different scenarios.

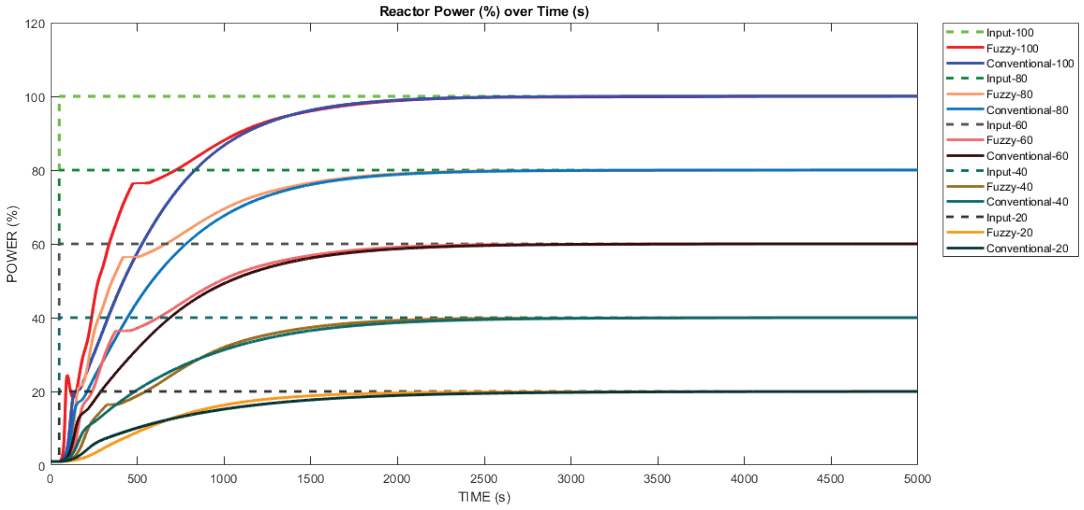

Fig. 4. Performance comparison of cCRSA and Fuzzy-CRSA in achieving different power demand levels.

TABLE III
SUMMARY OF RESULTS: COMPARISON BETWEEN FUZZY-CRSA AND CCRSA

PERFORMANCE	CCRSA	FUZZY-CRSA	COMPARISON (FUZZY-CRSA VS CCRSA)	IMPROVEMENT PERCENTAGE IN FUZZY-CRSA (%)
POWER DEMAND – 100%				
RISE TIME(S)	1.0083×10^{3}	1.0026×10^{3}	5.7	0.57
SETTLING TIME(S)	1.7586×10^{3}	1.7984×10^{3}	−39.8	−2.26
OVERSHOOT (%)	7.5823×10^{-7}	5.1549×10^{-6}	-4.39667×10^{-6}	−580
PEAK TIME(S)	4.9995×10^{3}	4.9999×10^{3}	−0.4	−0.01
POWER DEMAND – 80%				
RISE TIME(S)	1.0782×10^{3}	0.9968×10^{3}	81.4	7.55
SETTLING TIME(S)	1.8892×10^{3}	1.8298×10^{3}	59.4	3.14
OVERSHOOT (%)	1.3304×10^{-6}	4.5827×10^{-6}	-3.2523×10^{-7}	−24.45
PEAK TIME(S)	4.9999×10^{3}	4.9999×10^{3}	0	0
POWER DEMAND – 60%				
RISE TIME(S)	1.1624×10^{3}	1.0683×10^{3}	94.1	8.10
SETTLING TIME(S)	2.0640×10^{3}	1.8988×10^{3}	165.2	8.00
OVERSHOOT (%)	2.4483×10^{-6}	3.3220×10^{-6}	-8.737×10^{-7}	−35.69
PEAK TIME(S)	4.9999×10^{3}	4.9999×10^{3}	0	0
POWER DEMAND – 40%				
RISE TIME(S)	1.2972×10^{3}	1.1552×10^{3}	142	10.95
SETTLING TIME(S)	2.2894×10^{3}	1.9854×10^{3}	304.3	13.29
OVERSHOOT (%)	3.1314×10^{-6}	3.2639×10^{-6}	-1.325×10^{-7}	−4.23
PEAK TIME(S)	4.9999×10^{3}	4.9999×10^{3}	0	0
POWER DEMAND – 20%				
RISE TIME(S)	1.4516×10^{3}	1.0500×10^{3}	401.6	27.67
SETTLING TIME(S)	2.6904×10^{3}	1.9936×10^{3}	696.4	25.88
OVERSHOOT (%)	2.0196×10^{-6}	4.7992×10^{-6}	-2.7796×10^{-6}	−137.63
PEAK TIME(S)	4.9999×10^{3}	4.9999×10^{3}	0	0

IV. Conclusion

In conclusion, the comprehensive evaluations and analyses revealed that the fuzzy logic-based approach using Fuzzy-CRSA outperformed the traditional cCRSA method. It consistently delivered faster step responses, including shorter rise and settling times, across various scenarios—except in the case of achieving 100% target power from an initial 1% power level. This exception may be attributed to a brief spike followed by a drop observed in the response.

Additionally, a thorough analysis of control rod movement and its impact on reaching desired reactor power levels was successfully conducted. By simulating various control rod movement scenarios and examining the resulting power outputs, valuable insights were gained into the critical relationship between control rod positioning and power generation efficiency.

These findings are significant for RTP reactor power control, highlighting the benefits of a fuzzy logic-based approach for control rod selection and movement. The MATLAB simulation model developed in this study provides a solid foundation for future research and optimization of control rod systems at RTP, offering a strong basis for advancing power control strategies.

ACKNOWLEDGEMENTS

The authors wish to acknowledge the Malaysian Nuclear Agency for providing RTP data and Universiti Putra Malaysia for supporting this research collaboration.

Conflict of Interest

The authors declare no conflict of interest in the publication process of the research article.

Author Contributions

Author 1: Responsible for data collection, analysis, and original draft preparation; Author 2: Provided supervision and guidance in the conceptual methodology and analysis of simulation results; Author 3: Contributed to conceptualization and review; Author 4: Provided technical guidance for real operation (RTP) and the simulation-based system.

References

[1] Malaysian Nuclear Agency, (2024, Nov, 13). Nuclear Reactor Technology. [Online]. Available: https://www.nuclearmalaysia.gov.my/eng/rndActivities.php.

[2] R.M.G.P. Souza and A.Z. Mesquita, "Neutronic tests in the IPR-R1 Triga Reactor," in *Proc. IAEA,* Rabat, Morocco, 2011, pp. 1-8.

[3] N. A. Abdullah, "Parameter estimation using particle swarm optimization in the designing of lead-lag compensator for reactor Triga Puspati, "Ph.D thesis, Depart. of Electrical & Electronic Eng., Univ. Putra Malaysia, Selangor, Malaysia, 2023.

[4] Westinghouse Technology Systems Manual, Section 8.1, Rod Control System. [Online]. Available: https://www.nrc.gov/docs/ML1122/ML11223A252.pdf

[5] H. K. Louis, R. M. Refeat, and M. I. Hassan, "Control rod shadowing effect in PWR core utilizing Urania-Gadolinia fuel," *Progress in Nuclear Energy*, vol. 142, Dec. 2021, doi: 10.1016/j.pnucene.2021.103993.

[6] M. S. Minhat, N. A. Mohd Subha, F. Hassan, and N. M. Nordin, "An improved control rod selection algorithm for core power control at Triga Puspati reactor," *Journal of Mechanical Engineering and Sciences*, vol. 14, no. 1, pp. 6362–6379, Mar. 2020, doi: 10.15282/jmes.14.1.2020.13.0498.

[7] M.S. Andraws, A.A. Abd, A.H. Yousef, Mahmoud II and S.A. Hammad, "Performance of receding horizon predictive controller for research reactor", in *Proc. ICCES*, Cairo, Egypt, 2017.

[8] N. I. Saleh, M. T. Ijab, and N. Hashim," A review on Industrial Revolution 4.0 (IR4. 0) readiness among industry players," in *Proc CITIC,* Kuala Lumpur, Malaysia, 2022, pp. 216-231.

[9] E. R. G. D. Ribeiro, D. A. P. Palma, E. Henrice and J. Su, "Transient analysis of the Brazilian multipurpose reactor by the coupled neutronics and thermal hydraulics code NTHC1," *Annals of Nuclear Energy*, vol. 143, no. 1, pp. 1– 11, Aug. 2020, doi: 10.1016/j.anucene.2020.107449.

[10] S. Talebi and P. Najafi," A two-phase model for simulation of MTR type research reactor during protected and unprotected LOFA," *Progress in Nuclear Energy*, vol. 110, pp. 274–288, Jan. 2019, doi: 10.1016/j.pnucene.2018.10.004.

[11] L. Wang, X. Wei, F. Zhao and X. Fu, "Modification and analysis of load follow control without boron adjustment for CPR1000, "Annals *of Nuclear Energy*, vol. 70, pp. 317–328, Aug. 2014, doi: 10.1016/j.anucene.2013.12.001.

[12] H.L. Akin and V. Altin, "Rule-based fuzzy logic controller for a PWR-type nuclear power plant," *IEEE Transactions on Nuclear Science*, vol. 38, no. 2, pp. 883–890, April 1991, doi: 10.1109/23.289405.

[13] F. Khoshahval and A. Aziz, "Determination of the maximum speed of WWER-1000 nuclear reactor control rods," *Annals of Nuclear Energy*, vol. 87, no. 2, pp. 58–68, Jan. 2016, doi: 10.1016/j.anucene.2015.06.044.